Spin Peierls Effect in Spin Polarization of Fractional Quantum Hall States

Shosuke Sasaki

Shizuoka Institute of Science and Technology 2200-2 Toyosawa Fukuroi, 437-8555, Japan

E-mail:sasaki@ns.sist.ac.jp, phone:+81-538-45-0191, fax:+81-538-45-0110

Electron spin polarizations have been measured in the fractional quantum Hall effect. In experimental curves, a number of plateaus appear, some that are wide and others that are narrow. In this paper, theoretical calculations are presented to explain these observations. In the Landau gauge, single electron orbitals have the shape of equally spaced parallel lines. When a specific electron configuration of these orbitals is considered, the minimum classical Coulomb energy is obtained. Residual Coulomb interactions produce spin exchange interactions. If the spin-Peierls effect (modulation of the intervals between orbitals) is also taken into consideration, a new small energy gap appears. The total energy resulting from this modulation is smaller than the total energy in the non-modulated case, indicating that the modulation actually occurs. Eigenenergies are calculated under this modulation. The calculated spin polarization curves then exhibit both narrow and wide plateaus, and are in good agreement with the experimental data.

Keywords: Equilibrium thermodynamics and statistical mechanics, Many body and quasi-particle theories, Hall effect, Magnetic phenomena, Surface electronic phenomena, Semiconductor-semiconductor heterostructures

1. Introduction

I. V. Kukushkin, K. von Klitzing and K. Eberl have measured the electron spin polarization in the fractional quantum Hall effect (FQHE) for twelve filling factors [1]. The results exhibit wide plateaus and small shoulders on the magnetic dependence curve of the spin polarization. Explaining this complicated spin-polarization behavior theoretically is difficult, although many theoretical investigations have been conducted into the fractional quantum Hall effect [2-5]. This behavior is investigated in this paper.

In the integral quantum Hall effect, Laughlin et al used the Landau gauge and clarified the quantization of Hall resistance [6, 7]. Tao and Thouless [8] adopted these states in FQHE, but the lowest order ground states were degenerate, so diagonalizing the Coulomb interactions is difficult.

In a previous paper [9], we divided the total Hamiltonian H_{T} into two parts as $H_{\mathrm{T}} = H_{\mathrm{D}} + H_{\mathrm{I}}$, where the new 0th order Hamiltonian H_{D} includes the classical Coulomb energy. Therefore, the 0th order ground state of many electrons has the minimum classical Coulomb energy, and is not degenerate in the eigenstates of H_{D}. For the filling factor $\nu = 2/3$ as an example, the most uniform distribution of electrons in the orbitals is the electron configuration shown in Fig. 1.

=== Fig.1 ===

This electron configuration has the minimum classical Coulomb energy. The most uniform electron configuration at each filling factor can also be determined.

2. Spin-Peierls effect and spin exchange interactions

As seen in the previous section, the most uniform electron configuration has the minimum value of the classical Coulomb energy, namely the diagonal elements of the Coulomb interactions. The residual Coulomb interactions produce the spin exchange interaction. We consider the nearest neighbor interactions, the strengths of which are ξ and η, as illustrated in Figure 1. Next, the mechanism of spin-Peierls transitions [10] is taken into consideration. For $\nu = 2/3$, there are two electrons inside each unit cell, as shown in Figure 1. We make the intervals between electron orbitals wide in the first unit-cell, narrow in the second unit-cell, and so on. The coupling constant of the nearest orbital pair then changes from the original value to two different values ξ and ξ', and the coupling constant of the second nearest orbital pair also changes from the original value to two values η and η', as illustrated in Figure 2.

=== Fig.2 ===

The form of the spin exchange interactions is $\left(\sigma_1^+ \sigma_2^- + \sigma_1^- \sigma_2^+\right)$ where σ^+ is the transformation operator from a spin down state to a spin up state, and σ^- is the Hermitian conjugate operator of σ^+. Therefore, the explicit form of the spin exchange interactions for $\nu = 2/3$ is

$$
\begin{aligned}
H = & \sum_{j=1,2,3\cdots} \left[\xi\left(\sigma_{4j-3}^+ \sigma_{4j-2}^- + \sigma_{4j-3}^- \sigma_{4j-2}^+\right) + \eta\left(\sigma_{4j-2}^+ \sigma_{4j-1}^- + \sigma_{4j-2}^- \sigma_{4j-1}^+\right) \right] + \\
& + \sum_{j=1,2,3\cdots} \left[\xi'\left(\sigma_{4j-1}^+ \sigma_{4j}^- + \sigma_{4j-1}^- \sigma_{4j}^+\right) + \eta'\left(\sigma_{4j}^+ \sigma_{4j+1}^- + \sigma_{4j}^- \sigma_{4j+1}^+\right) \right] + \\
& + \sum_{j=1,2,3\cdots} \frac{\mu_B g}{\mu_0} B \frac{1}{2}\left(\sigma_{4j-3}^z + \sigma_{4j-2}^z + \sigma_{4j-1}^z + \sigma_{4j}^z\right)
\end{aligned}
\tag{1}
$$

where g is the g-factor, B is the magnetic field strength, σ^z is the electron spin operator in the z-direction, μ_0 is the permeability of free space and μ_B is the Bohr magneton. When

the interval modulation value d is small, the increasing value of the classical Coulomb energy is proportional to d^2, and the decreasing value of spin exchange energy is proportional to $|d|$ because of the gap production. Therefore, the total energy with the modulation present is smaller than in the non-modulation case for small modulations d. Consequently, the modulation actually occurs.

The Hamiltonian (1) can be rewritten by replacing the spin down state $|\Downarrow\rangle$ with the vacuum state $|0\rangle$, and the spin up state $|\Uparrow\rangle$ with the one fermion state $c*|0\rangle$, giving

$$H = \sum_{j=1,2,3\cdots}\left[\xi\left(c^*_{4j-3}c_{4j-2} - c_{4j-3}c^*_{4j-2}\right) + \eta\left(c^*_{4j-2}c_{4j-1} - c_{4j-2}c^*_{4j-1}\right)\right] +$$
$$+ \sum_{j=1,2,3\cdots}\left[\xi'\left(c^*_{4j-1}c_{4j} - c_{4j-1}c^*_{4j}\right) + \eta'\left(c^*_{4j}c_{4j+1} - c_{4j}c^*_{4j+1}\right)\right] + \sum_{i=1,2,3\cdots}\frac{\mu_B g}{\mu_0}B\frac{1}{2}\left(2c^*_i c_i - 1\right) \tag{2}$$

where the operators c_i and c^*_i are the annihilation and creation operators of a fermion. These procedures are described in reference [11]. The operators c_i and c^*_i are renumbered using the cell number j as follows:

$$a_{1,j} = c_{4j-3}, \quad a_{2,j} = c_{4j-2}, \quad a_{3,j} = c_{4j-1}, \quad a_{4,j} = c_{4j} \tag{3}$$

Fourier transformation gives

$$a_{1,j} = \frac{1}{\sqrt{J}}\sum_p e^{ipj}a_1(p), \quad a_{2,j} = \frac{1}{\sqrt{J}}\sum_p e^{ipj}a_2(p),$$
$$a_{3,j} = \frac{1}{\sqrt{J}}\sum_p e^{ipj}a_3(p), \quad a_{4,j} = \frac{1}{\sqrt{J}}\sum_p e^{ipj}a_4(p) \tag{4}$$

where $p = \frac{2\pi}{J} \times$ integer , $-\pi < p \le \pi$ and J is the total number of cells. Substituting (4) into (2) gives:

$$H = \sum_p\left[\begin{array}{l}\xi\left(a^*_1(p)a_2(p) + a^*_2(p)a_1(p)\right) + \eta\left(a^*_2(p)a_3(p) + a^*_3(p)a_2(p)\right) + \\ + \xi'\left(a^*_3(p)a_4(p) + a^*_4(p)a_3(p)\right) + \eta'\left(e^{ip}a^*_4(p)a_1(p) + e^{-ip}a^*_1(p)a_4(p)\right)\end{array}\right]$$
$$+ \sum_p\frac{\mu_B g}{\mu_0}B\frac{1}{2}\left(2\left(a^*_1(p)a_1(p) + a^*_2(p)a_2(p) + a^*_3(p)a_3(p) + a^*_4(p)a_4(p)\right) - 4\right) \tag{5}$$

The eigenenergies of Hamiltonian (5) for each wave number p are equal to the eigenvalues of

the matrix M as

$$
M = \begin{pmatrix}
\mu_B gB/\mu_0 & \xi & 0 & \eta' e^{-ip} \\
\xi & \mu_B gB/\mu_0 & \eta & 0 \\
0 & \eta & \mu_B gB/\mu_0 & \xi' \\
\eta' e^{ip} & 0 & \xi' & \mu_B gB/\mu_0
\end{pmatrix}
\tag{6}
$$

The eigenvalues $\lambda_1(p)$, $\lambda_2(p)$, $\lambda_3(p)$ and $\lambda_4(p)$ of this matrix M give the following

electron spin-polarization γ_e (see reference [11] for details):

$$
\gamma_e = \frac{1}{8\pi} \int_{-\pi}^{\pi} dp \left(\sum_{s=1}^{4} \tanh\left(\lambda_s(p)/2k_B T\right) \right).
\tag{7}
$$

There are random potentials in real Hall devices, which produce some fluctuations in the

eigenvalues. Replacing the random potential effect with a thermal vibration effect is assumed

to be a good approximation. Effective temperature T is then introduced. Next, we assume that

the ratio ξ'/ξ is equal to the ratio η'/η, because the modulation effect on the coupling

constant ξ may be the same as for η. Adopting the values $\eta/\xi = 0.1$ $\xi'/\xi = \eta'/\eta = 1.4$ and

$(k_B T/\xi) = 0.05$, a small energy gap appears owing to the interval modulation and then a small

shoulder occurs in the electron spin-polarization curve, as shown in Figure 3.

=== Fig.3 ===

Experimental data shown in this figure was measured by I. V. Kukushkin, K. von Klitzing

and K. Eberl [1]. The theoretical curve agrees well with the experimental data. In the next

section, electron spin-polarizations are calculated for other values of filling factor.

3. Values of electron spin-polarization calculated for various filling factors

The most uniform distribution of electrons is found for the filling factors $\nu=3/5$ and $\nu=4/7$.

The electron configurations are shown in Figs. *4a* and *b*.

=== Fig.4a ===   === Fig.4b ===

These spin-exchange interactions give matrices (8) and (9) as

$$
\begin{pmatrix}
\mu_B gB/\mu_0 & \xi & 0 & 0 & 0 & \eta'e^{-ip} \\
\xi & \mu_B gB/\mu_0 & \eta & 0 & 0 & 0 \\
0 & \eta & \mu_B gB/\mu_0 & \eta & 0 & 0 \\
0 & 0 & \eta & \mu_B gB/\mu_0 & \xi' & 0 \\
0 & 0 & 0 & \xi' & \mu_B gB/\mu_0 & \eta' \\
\eta'e^{ip} & 0 & 0 & 0 & \eta' & \mu_B gB/\mu_0
\end{pmatrix}
\quad \text{(for } \nu=3/5) \qquad (8)
$$

$$
\begin{pmatrix}
\mu_B gB/\mu_0 & \xi & 0 & 0 & 0 & 0 & 0 & \eta'e^{-ip} \\
\xi & \mu_B gB/\mu_0 & \eta & 0 & 0 & 0 & 0 & 0 \\
0 & \eta & \mu_B gB/\mu_0 & \eta & 0 & 0 & 0 & 0 \\
0 & 0 & \eta & \mu_B gB/\mu_0 & \eta & 0 & 0 & 0 \\
0 & 0 & 0 & \eta & \mu_B gB/\mu_0 & \xi' & 0 & 0 \\
0 & 0 & 0 & 0 & \xi' & \mu_B gB/\mu_0 & \eta' & 0 \\
0 & 0 & 0 & 0 & 0 & \eta' & \mu_B gB/\mu_0 & \eta' \\
\eta'e^{-ip} & 0 & 0 & 0 & 0 & 0 & \eta' & \mu_B gB/\mu_0
\end{pmatrix}
\quad \text{(for } \nu=4/7) \quad (9)
$$

Electron spin polarizations are calculated from the eigenvalues of the matrices, and the results are shown in Figs. *5a* and *b*.

=== Fig. 5a ===   === Fig.5b ===

When we search the many electron states with the most uniform distribution for the three cases of $\nu=2/5$, $\nu=3/7$ and $\nu=4/9$, we find the electron configurations shown in Figs. *6a, b* and *c*. As can be seen from Fig. *6a*, one empty orbital exists between the first and second electrons from left to right, and then two empty orbitals exist between the second and third electrons. Four different coupling constants, η, η', ς and ς', thus exist under interval modulation, namely the spin-Peierls effect.

=== Fig. 6a ===

=== Fig. 6b ===

=== Fig. 6c ===

In these three cases, we write the matrix for $\nu=3/7$ as an example:

$$\begin{pmatrix} \mu_{\mathrm{B}}gB/\mu_0 & \eta & 0 & 0 & 0 & \varsigma'e^{-ip} \\ \eta & \mu_{\mathrm{B}}gB/\mu_0 & \eta & 0 & 0 & 0 \\ 0 & \eta & \mu_{\mathrm{B}}gB/\mu_0 & \varsigma & 0 & 0 \\ 0 & 0 & \varsigma & \mu_{\mathrm{B}}gB/\mu_0 & \eta' & 0 \\ 0 & 0 & 0 & \eta & \mu_{\mathrm{B}}gB/\mu_0 & \eta' \\ \varsigma'e^{ip} & 0 & 0 & 0 & \eta' & \mu_{\mathrm{B}}gB/\mu_0 \end{pmatrix} \quad \text{(for } \nu=3/7) \qquad (10)$$

The calculated electron spin polarizations are plotted in Fig. 7a, 7b, and 7c.

=== Fig.7a ===   === Fig.7b ===   === Fig.7c ===

The three cases of filling factors $\nu=4/3$, 7/5, and 8/5 are also considered. In these cases, the

most uniform distribution is realized by the electron configurations shown in Fig. 8.

=== Fig.8a ===

=== Fig.8b ===

=== Fig.8c ===

As can easily be seen from these figures, pairs of electrons with up and down spins occupy

single orbitals in the orbitals drawn as double lines. Spin cannot flip in the double line states

because of Pauli's exclusion principle. Therefore, spin exchange forces act only between pairs

of electrons in single line orbitals (see Fig. 8). Taking these situations into consideration,

electron spin polarization curves can be calculated. The results are shown in Fig. 9.

=== Fig.9a ===   === Fig.9b ===   === Fig.9c ===

4. Results and discussions

As can be seen in Figs. 3, 5, 7, and 9, the calculated electron spin polarization curves have small shoulders, which are caused by interval modulation, namely the spin-Peierls effect. Small shoulders also appear in the data of Kukushkin et al [1], and our calculated curves are in good agreement with the experimental data. Thus, the spin-Peierls effect can be concluded to appear in the electron spin polarization of the fractional quantum Hall effect.

References

[1] I. V. Kukushkin, K. v. Klitzing, and K. Eberl, Phys.Rev.Lett.**82** (1999) 3665.

[2] R. B. Laughlin, Phys. Rev. Lett. **50** (1983) 1359.

[3] F. D. M. Haldane, Phys. Rev. Lett. **51** (1983) 605.

[4] R. B. Laughlin, Phys. Rev. B**27** (1983) 3383.

[5] J. K. Jain, Phys. Rev. Lett. **63** (1989) 199.

[6] R. B. Laughlin, Phys. Rev. B**23** (1981) 5632.

[7] B. I. Halperin, Phys. Rev. B**25** (1982) 2185.

[8] R. Tao and D. J. Thouless, Phys. Rev. **B 28** (1983) 1142; R. Tao, Phys. Rev. **B 29** (1984) 636.

[9] S. Sasaki, Physica **B 281** (2000) 838. S. Sasaki, Proc. 25th Int. Conf. Phys. Semicond., (Springer 2001) 925.

[10]   R. E. Peierls, Quantum Theory of Solids (Oxford University, London, 1955).

[11]   S. Sasaki, Phys. Rev. **E, 53** (1996) 168.

Figure captions

Fig.1 Electron configuration at the minimum Coulomb energy for $\nu = 2/3$ (dashed lines are empty orbitals)

Fig. 2 Coupling constants of spin exchange interactions caused by interval modulation

Fig. 3 Calculated curve of the spin-polarization for $\nu = 2/3$ (Dots are experimental data)

Fig. 4a Coupling constants for $\nu=3/5$.   Fig. 4b Coupling constants for $\nu=4/7$.

Fig. 5a Spin polarization for $\nu=3/5$.   Fig. 5b Spin polarization for $\nu=4/7$.

Fig. 6a Electron configuration for $\nu=2/5$

Fig. 6b Electron configuration for $\nu=3/7$

Fig. 6c Electron configuration for $\nu=4/9$

Fig. 7a Spin polarization for $\nu=2/5$

Fig. 7b Spin polarization for $\nu=3/7$

Fig. 7c Spin polarization for $\nu=4/9$

Fig. 8a Electron configuration for $\nu=4/3$. Double lines present pairs of electrons with up and down spins.

Fig. 8b Electron configuration for $\nu=7/5$

Fig. 8c Electron configuration for $\nu=8/5$

Fig. 9a Spin polarization for $\nu=4/3$

Fig. 9b Spin polarization for $\nu=7/5$

Fig. 9c Spin polarization for $\nu=8/5$

Fig.1

Fig.2

$\xi^{'}/\xi= \eta^{'}/\eta=1.4$

$\eta/\xi=0.1$

$\kappa_{B}T /\xi=0.05$

$\nu=2/3$

Polarization

Magnetic field strength (T)

Fig.3

Fig.4a

Fig.4b

$\xi'/\xi = \eta'/\eta = 1.25$

$\eta/\xi = 0.52$

$\kappa_B T /\xi = 0.05$

$\nu = 3/5$

Fig.5a

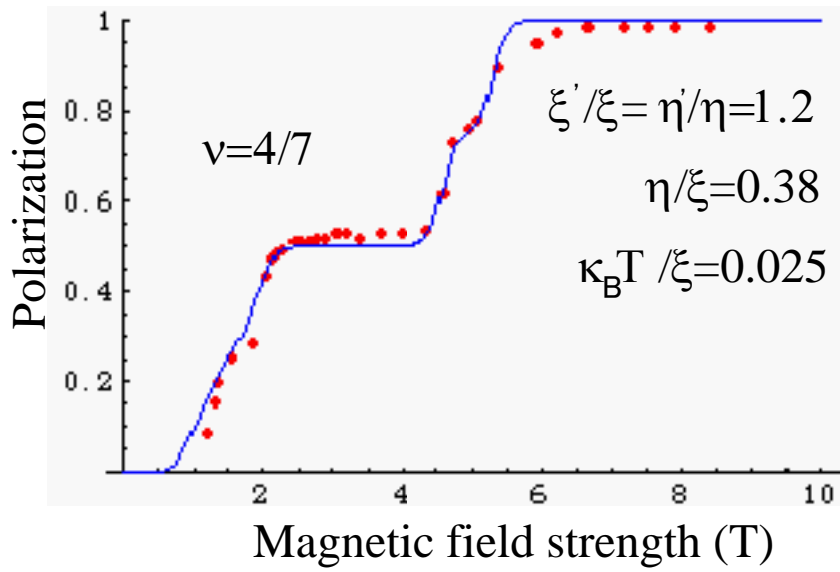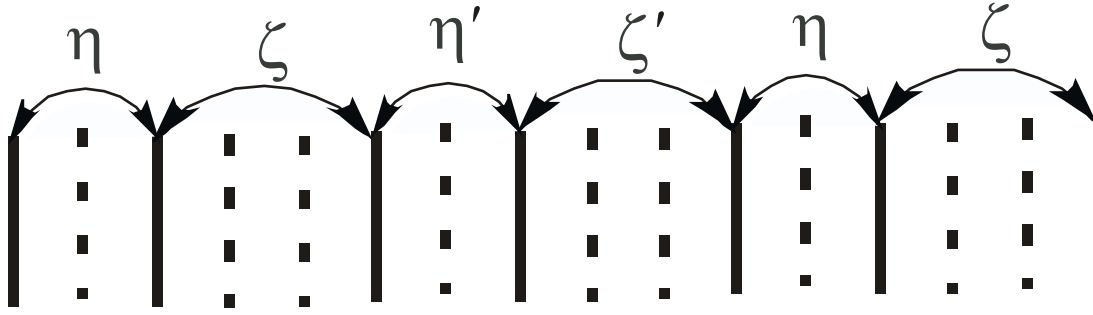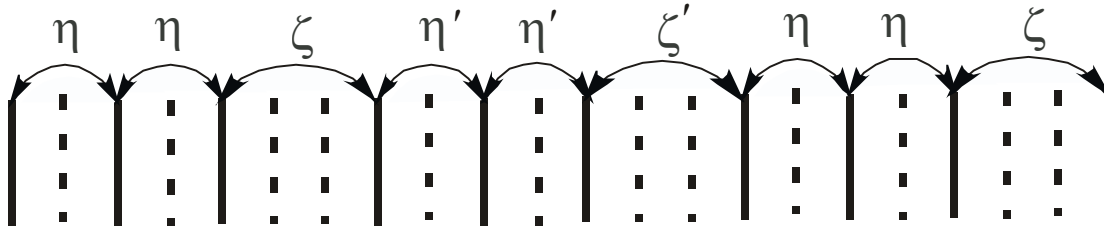$\xi'/\xi = \eta'/\eta = 1.2$

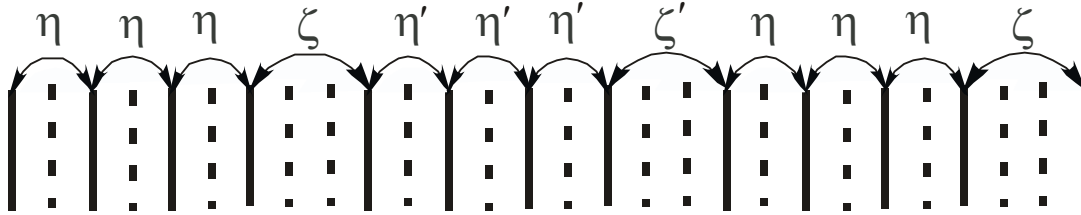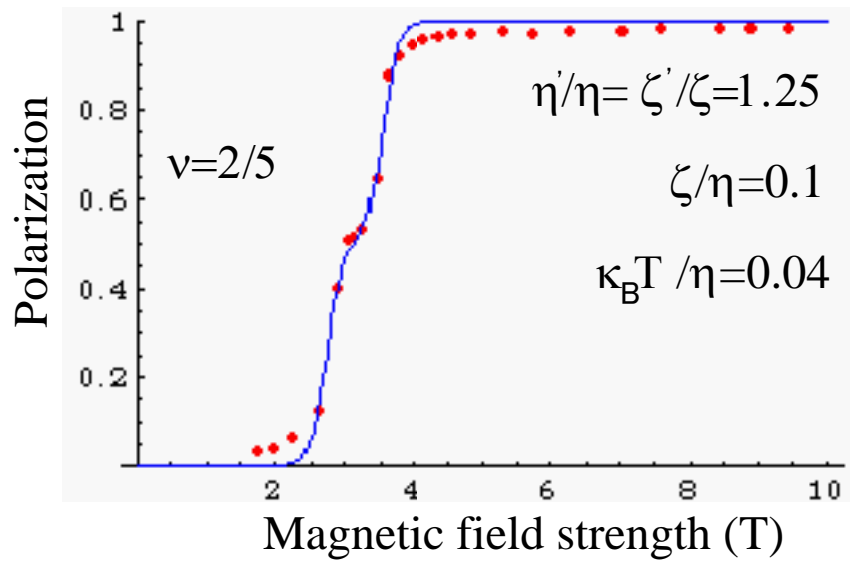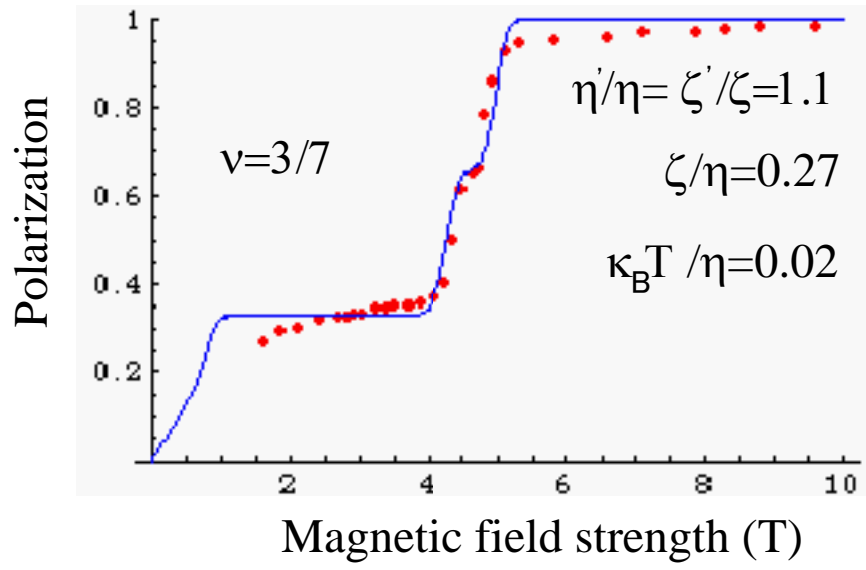$\eta/\xi = 0.38$
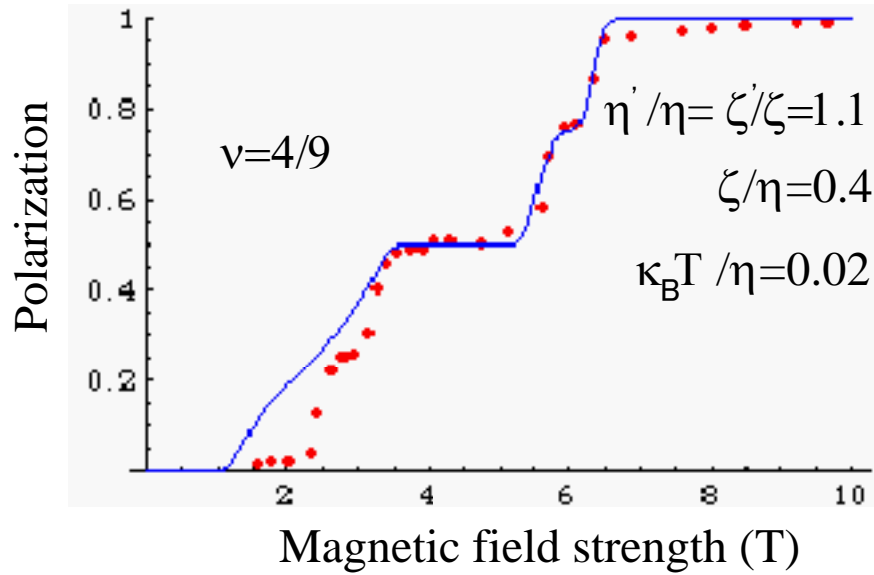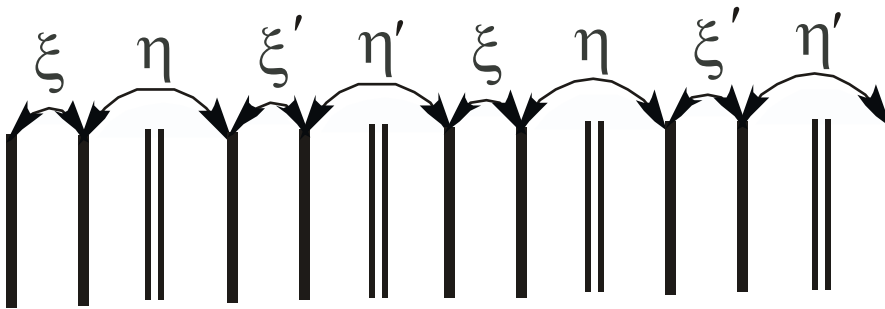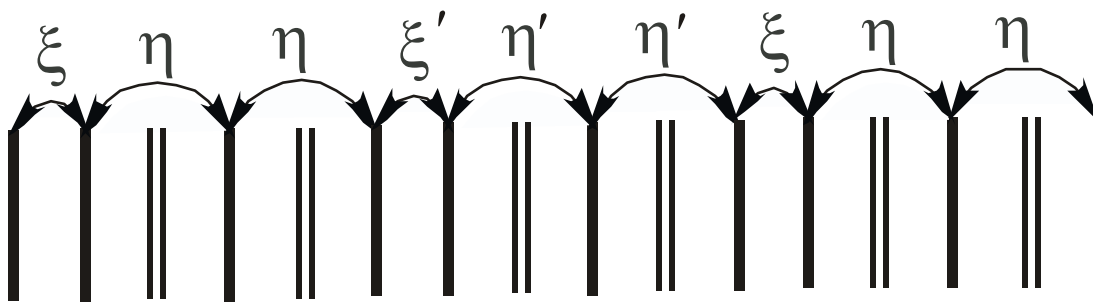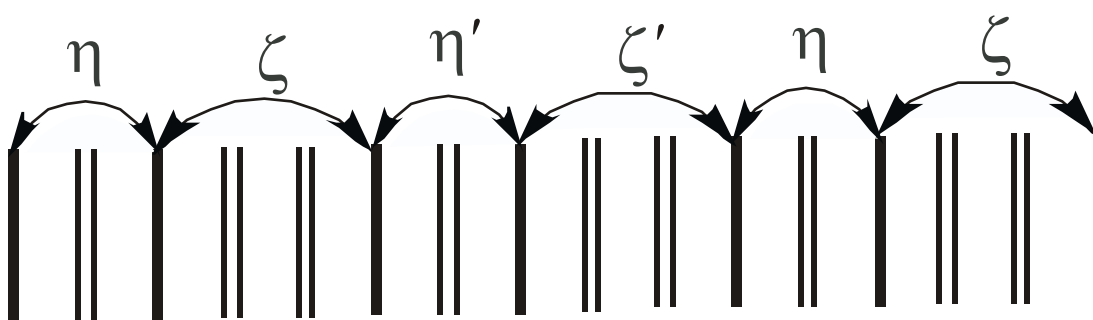
$\kappa_B T /\xi = 0.025$

$\nu = 4/7$
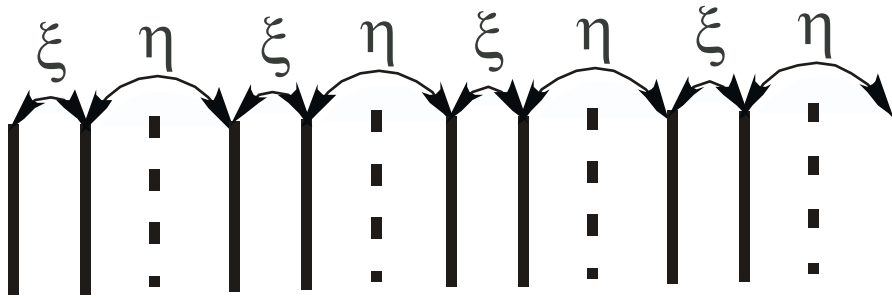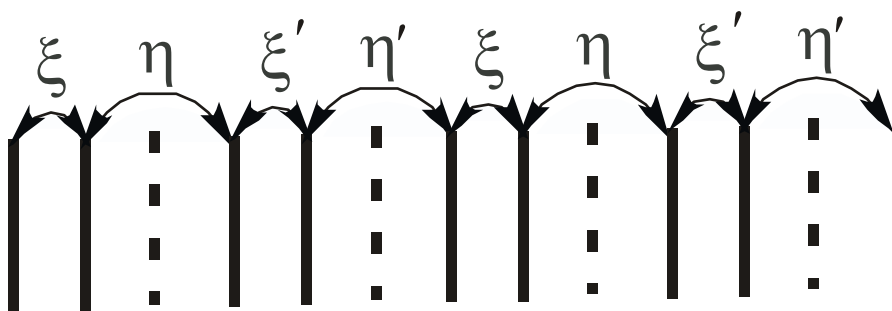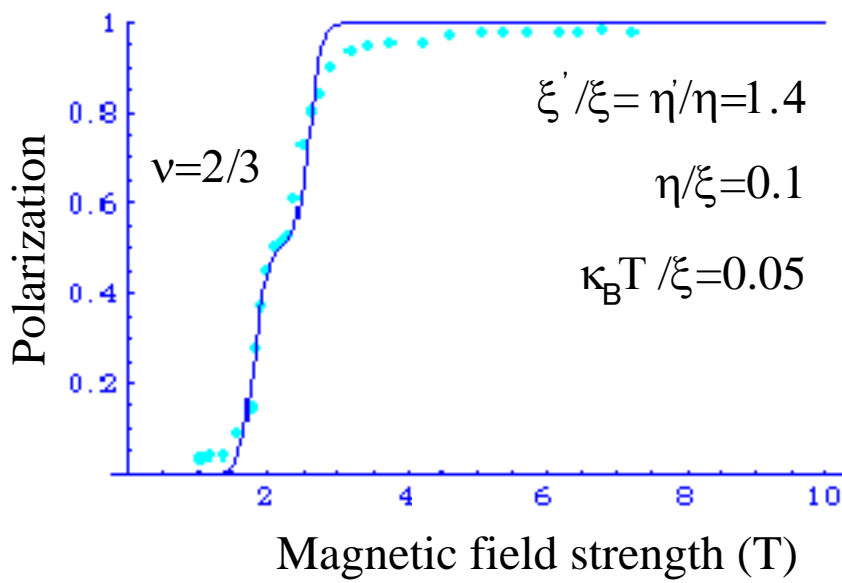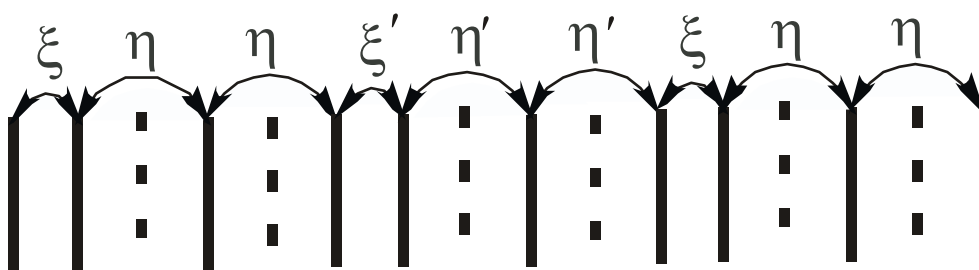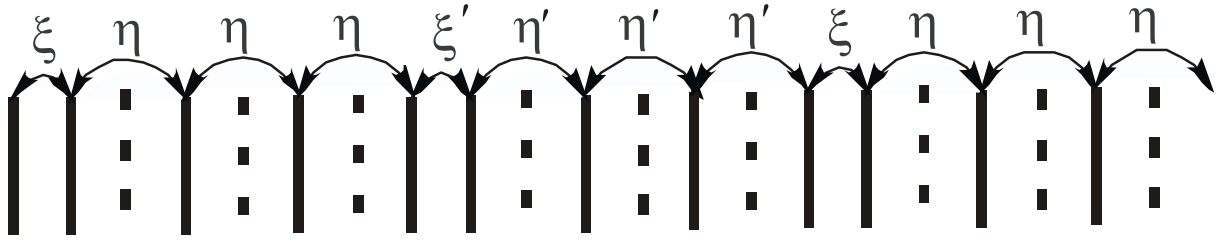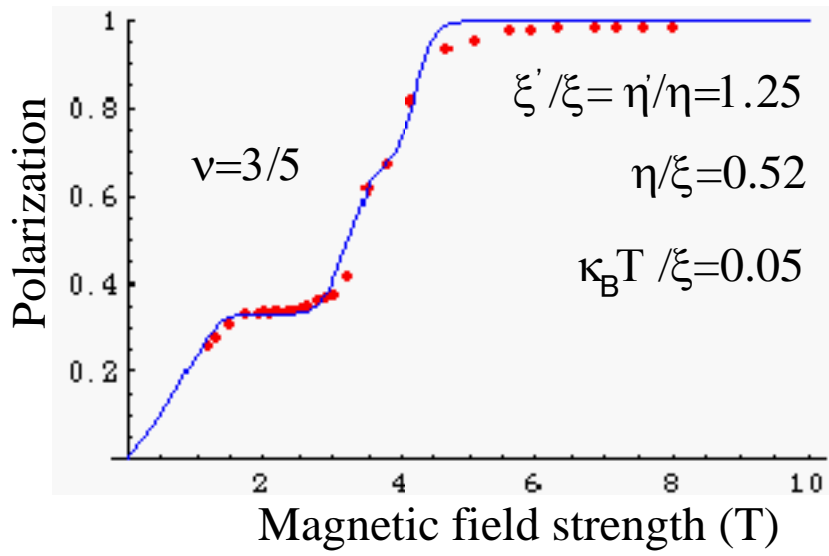
Fig.5b

Fig.6a

Fig.6b

Fig.6c

Fig.7a

Fig.7b

Fig.7c

Fig.8a

Fig.8b

Fig.8c

$\xi'/\xi = \eta'/\eta = 1.1$

$\eta/\xi = 0.1$

$\kappa_B T/\xi = 0.02$

$\nu = 4/3$

Polarization

Magnetic field strength (T)

Fig.9a

$\xi'/\xi = \eta'/\eta = 1.2$

$\eta/\xi = 0.1$

$\kappa_B T /\xi = 0.035$

$\nu = 7/5$

Magnetic field strength (T)

Fig.9b

$\eta'/\eta = \zeta'/\zeta = 1.1$

$\zeta/\eta = 0.1$

$\kappa_B T /\eta = 0.025$

$\nu = 8/5$

Magnetic field strength (T)

Fig.9c